Automated Update of an Irrigated Lands GIS Using SPOT HRV Imagery

David W. Eckhardt and *James P. Verdin*
Bureau of Reclamation, Research and Laboratory Services Division, Denver, CO 80225
Gordon R. Lyford
Bureau of Reclamation, Mid-Pacific Regional Office, Sacramento, CA 95825

ABSTRACT: The Bureau of Reclamation (Reclamation) has created and maintains a geographic information system (GIS) for the Newlands irrigation project in west-central Nevada. Reclamation has developed a method for updating the irrigation status attribute of individual agricultural fields within this GIS using digital imagery acquired by spaceborne sensors. This method includes registration of one or more images each year to a Universal Transverse Mercator grid system, image normalization, transformation of the imagery into Brightness and Greenness spectral features, and pixel-by-pixel classification of the transformed imagery into irrigated and not irrigated classes. Digital overlay of the field boundary data onto the classified imagery is then performed to determine the irrigation status of each individual field, based upon the values of the pixels it contains. Satellite imagery is also used to identify new agricultural fields to be added to the geographic data base.

INTRODUCTION

THE NEWLANDS PROJECT is located in west-central Nevada and contains approximately 25,000 hectares of irrigated lands (Figure 1 and Plate 1). Pasture and alfalfa are the primary crops, but there are significant areas of grain, corn, and truck crops. The project is located at an elevation of 1200 metres in the rain shadow of the Sierra Nevada, with an average annual rainfall of less than 150 millimetres. Lahontan Reservoir, which supplies the project, is fed primarily by snowmelt runoff from the Carson River and is supplemented by a trans-basin diversion from the Truckee River. Both rivers originate in the Sierra Nevada.

The trans-basin diversion of water, and competition for water between farmers, indian tribes, cities, and wildlife interests, has led to numerous lawsuits. These lawsuits prompted the courts to direct the U.S. Bureau of Reclamation (Reclamation) to develop Operating Criteria and Procedures (OCAP) for the project. The OCAP specify project operations to minimize Truckee River diversions while ensuring that water right entitlements are satisfied. These project operations are based on estimates of hydrologic conditions, such as snow pack and reservoir storage, and irrigation water demand for the coming irrigation season.

Snowmelt runoff for the Carson and Truckee watersheds is estimated from snow course data, and reservoir storage is estimated using reservoir elevation/volume tables. Irrigation water demand for the coming irrigation season is predicted by modifying estimates of the previous year's maximum irrigation water demand. This modification is based primarily upon water right transfers approved by the Nevada State Engineer that will take effect during the coming season.

Reclamation has constructed and maintains a geographic information system (GIS) for the project (Verdin *et al.*, 1985) which is used to calculate maximum irrigation water demand for previous years. Data themes within this GIS include land ownership, sections and quarter-quarter sections of the U.S. Public Land Survey System (PLSS), agricultural fields, water rights, and bench- and bottom-land soil designations. The land ownership, PLSS, water rights, and soil type data layers were digitized into the GIS from existing maps. The agricultural fields data theme was generated from 1:24,000-scale aerial photography acquired during the 1984 growing season. All data themes were reconciled to the PLSS theme to reduce misregistration between themes.

The previous year's maximum irrigation water demand is calculated by using the GIS to sum the area of all irrigated, water righted fields, multiplied by their maximum irrigation water allocation (determined by the bench- or bottom-land soil designation). The land ownership and PLSS data themes are used to aggregate spatially this water demand information. Because irrigation patterns within the project change from year to year, the "irrigated" or "not irrigated" attribute for each agricultural field within the data base must be updated annually.

This paper describes how images acquired in 1987 and 1988 by the High Resolution Visible (HRV) sensors aboard the Systeme Probatoire d'Observation de la Terre (SPOT) satellite were used to provide this attribute and to locate new agricultural fields brought into production since the initial mapping of agricultural fields in 1984. Both image processing and GIS procedures are described in detail, with particular attention given to scene normalization techniques. Although SPOT HRV data were used in this project, the methods developed here are usable with data acquired by other spaceborne sensors.

METHODS AND RESULTS

PROVIDING IRRIGATION ATTRIBUTES FOR DIGITIZED FIELDS

A digital overlay analysis procedure was used to obtain an irrigated or not irrigated attribute for each individual field within the study area. HRV images from May and August of 1987 and 1988 were first normalized to match environmental conditions of a July 1986 reference scene, then were transformed into Brightness and Greenness images. These images were classified on a pixel-by-pixel basis into irrigated and not irrigated classes. The irrigated field polygons stored within the GIS were then rasterized and overlaid on the classified images. The irrigation status of each field was determined from the irrigation class values of its pixels. Image processing procedures will be described first, followed by a description of the digital overlay procedure, and a discussion of the results.

Image Processing Procedures

Multispectral images acquired by the two High Resolution Visible sensors (HRV1 and HRV2) aboard the SPOT satellite were chosen as the data source for this project primarily due to their relatively small (20-metre at nadir) pixel size, and spectral bands that are well suited to monitoring green vegitation (Table 1) . The image processing segment of this work consisted of five

PHOTOGRAMMETRIC ENGINEERING & REMOTE SENSING,
Vol. 56, No. 11, November 1990, pp. 1515–1522.

0099-1112/90/5611–1515$03.00/0

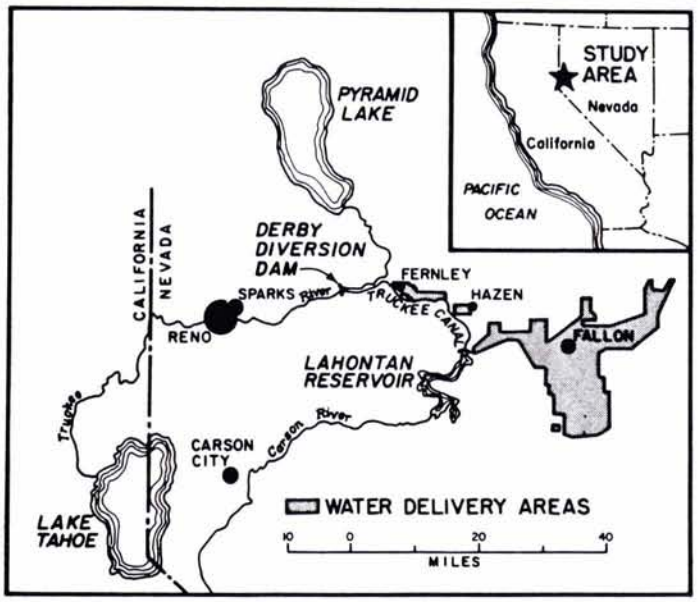

FIG. 1. Location of the Newlands Project.

TABLE 1. SPOT HRV SPECTRAL BANDS (MULTISPECTRAL (XS) MODE).

Spectral Band	Wavelength Range (micrometres)	Description
XS1	0.50 – 0.59	green
XS2	0.61 – 0.68	red
XS3	0.79 – 0.89	near infrared

TABLE 2. SPOT HRV SCENES USED FOR IRRIGATED LANDS MONITORING.

Acquisition date	14 Jul 86	11 May 87	14 Aug 87	21 May 88	21 Aug 88
Local time (PDT)	11:56:03	12:06:33	11:39:56	11:35:16	12:06:47
Sensor	HRV2	HRV1	HRV2	HRV2	HRV1
Incidence angle	L 1.7	L 20.2	R 22.3	R 27.2	L 20.9
Solar elevation	67.4	66.1	59.7	64.7	60.5
Solar azimuth	136.2	152.3	138.7	134.0	153.7
Number of lines	3003	3006	2995	2992	3005
Number of pixels per line	2989	3363	3458	3718	3394
Across track pixel dimension	20.0m	22.4m	23.1m	24.8m	22.6m

TABLE 3. NEWLANDS PROJECT GEOGRAPHIC GRID SYSTEM.

Map projection:	UTM
Zone:	11
Grid origin:	
Center of 0,0 pixel in upper left corner:	4393500N 303500E
Lower left corner of lower left pixel:	4349890N 303510E
Cell size:	20 metres
Number of lines (rows):	2180
Number of samples (columns):	3600

steps: image acquisition, registration, normalization, transforamtion, and classification.

Image Acquisition

In addition to an HRV scene that had been acquired in July 1986, a total of four scenes was acquired in May and August of 1987 and 1988 (Table 2). The decision to use imagery acquired in May and August was based primarily upon knowledge of the phenology of alfalfa, the most prevalent crop in the project. The May and August dates were chosen to reveal a maximum number of fields with a detectable crop cover.

The off-nadir viewing capability of SPOT allows for frequent image acquisition opportunities that are often critical in agricultural remote sensing. Although off-nadir viewing increases pixel size in the across-track direction by up to 35 percent, this increased pixel size also affords imaging areas up to 35 percent larger than the 60- by 60-kilometre area imaged at nadir (CNES, 1988). Because the Newlands Project area is more than 60 kilometres east-west, only images acquired with an off-nadir look angle of at least 17 degrees were purchased. If properly positioned, images acquired at a 17 degree or greater look angle are large enough to contain the entire study area. However, the fixed 0.6 degree increments in which the HRV sensor can point off-nadir were not always fine enough to position the image squarely on the study area (CNES, 1988). As a result, approximately three percent of the study area had no image coverage for 1988.

Image Registration

The HRV images were resampled to a Universal Transverse Mercator grid having a 20-metre cell size and encompassing the entire Newlands Project area (Table 3). Ground control points were selected from U.S. Geological Survey 7½-minute topographic maps and orthophoto quadrangles. Although there was significant relief displacement in high relief areas due to large off-nadir look angles, there was little geometric distortion in the relatively flat agricultural areas. First-order polynomial equations were used to define the relationship between the image and project grid systems. The maximum root-mean-square (RMS) error of the 11 to 13 control points used to register each of the scenes was 0.35 pixel. A cubic convolution resampling kernel was used during image registration.

Image Normalization

The ability to use HRV images to assign a reliable irrigated or not irrigated attribute to an agricultural field is contingent upon there being a robust relationship between HRV pixel digital numbers (DNs) and surface conditions. However, factors such as sun angle, Earth/sun distance, detector calibration of the two HRV sensors, atmospheric condition, and sun/target/sensor geometry (phase angle) will also affect pixel DNs. Image normalization was undertaken to reduce pixel DN variation caused by non-surface factors, so that variations in pixel DN between dates could be related to actual changes in surface conditions. Normalization enabled the use of pixel classification rules developed from one HRV scene to be applied reliably to other HRV scenes.

Differences in direct beam solar radiation due to variation in sun angle and Earth/sun distance can be calculated accurately, as can variation in pixel DNs due to detector calibration differences between HRV sensors. However, removal of atmospheric and phase angle effects require information about the gaseous and aerosol composition of the atmosphere and the bidirectional reflectance characteristics of elements within the scene. Because atmospheric and bidirectional reflectance information was not available for any of the four HRV scenes, an empirical scene normalization approach was employed in an attempt to match the detector calibration, astronomic, atmospheric, and phase angle conditions present in a reference scene.

The 14 July 1986 HRV scene was selected as the reference

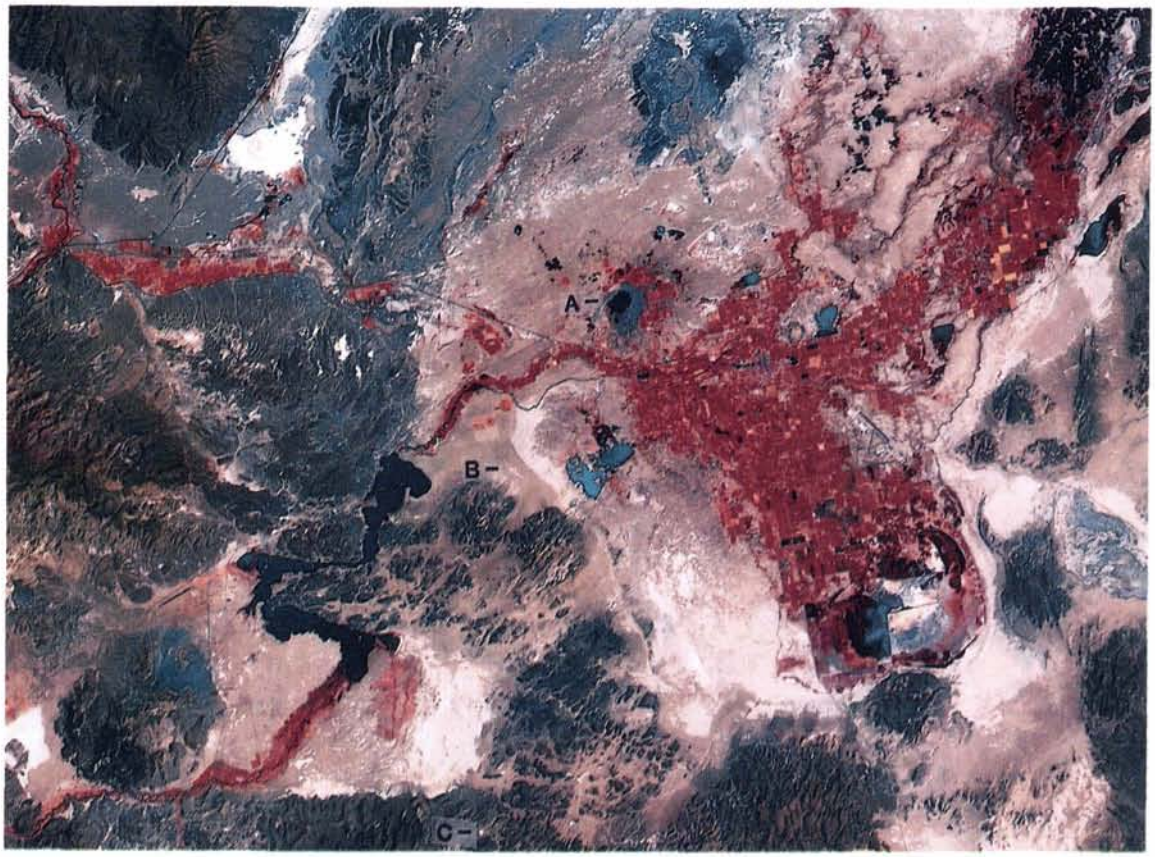

PLATE 1. Thematic Mapper scene showing the location of scene normalization targets adjacent to the Newlands Project. A: Soda Lake B: Badlands C: Dry Lake Bed

scene to which the 1987 and 1988 scenes were normalized. This scene was chosen as the standard because it had the highest sun angle of any image of the study area held by Reclamation, and because it was acquired with an incidence angle of less than 2° left (east) of nadir. This small look angle minimized the amount of atmospheric attenuation and haze present in the scene.

Image normalization was achieved by applying regression equations to the 1987 and 1988 imagery which predict what a given pixel's DN would be if it had been acquired under the same conditions as the 1986 reference scene. These regression equations were developed by matching the DNs of normalization targets present in both the scene being normalized and the reference scene. Normalization targets were assumed to be constant reflectors, so any changes in their DNs between dates were attributed to detector calibration, astronomic, atmospheric, and phase angle differences. Once these variations were removed, changes in DN could be related to changes in surface conditions.

The acceptance criteria for potential normalization targets were

- The target must be at approximately the same elevation as the irrigated lands within the scene. Because most of the aerosols in the atmosphere typically occur within the lowest 1000 metres, choosing a mountaintop normalization target would be of little use in estimating atmospheric conditions at lower elevations.
- The target can contain only minimal amounts of vegetation. Vegetation spectral reflectance can change over time due to environmental stresses and plant phenology.
- The target must be in a relatively flat area so that incremental changes in sun angle from date to date will have the same proportional increase or decrease in direct beam sunlight for all normalization targets.
- When viewed on the image display screen, the patterns seen on normalization targets should not change over time. Changing patterns indicate a variability within the target which could mean that the reflectance of the target as a whole may not be constant over time. For example, a mottled pattern on what had previously been a continuous tone dry lake bed indicates changing surface moisture conditions, which would eliminate the dry lake bed from consideration as a normalization target.

Besides selecting targets that met the four conditions listed above, efforts were made to select a set of targets exhibiting a wide range of pixel brightness values. Regression models developed from a wide range of data values are generally better predictors than those developed from data with a smaller range.

Fourteen candidate constant reflectance targets were tested and only three met the acceptance criteria. Fortunately, these three targets spanned a wide range of DNs. Soda Lake, a deep, clear lake fed by underground springs, served as a dark normalization target. The two brighter targets were a badlands area located approximately 8 kilometres east of the Lahontan Reservoir Dam, and a dry lake bed in the Desert Mountains in the southern part of the study area (Plate 1).

Normalization DNs were obtained from a video display screen. For the dark normalization target, Soda Lake, the normalization DN for a scene was defined as the lowest DN having at least 50 pixels at that value or below. Similarly, the two bright normalization DNs were obtained by choosing DNs having at least 10 pixels at that value or above. Mean values for the bright nor-

malization targets were not used because variations in target boundary identification were possible due to slight date-to-date misregistrations. Such misregistrations might result in significant changes in the mean value of either bright target due to their rather small size (as few as 70 pixels). Manually refining these boundaries would introduce a subjective element into the process which would affect the mean values. Using the mean value for the Soda Lake target was not pursued initially because of the perceived possibility of specular reflection of sunlight by waves from parts of the lake surface. This problem did not materialize, however. Extreme high or low DNs from normalization targets were not used because they might have resulted from image noise, artifacting at high contrast interfaces from the cubic convolution resampling algorithm (Verdin, 1983), or, for the smaller terrestrial targets, differing pixel compositions from scene to scene.

Twelve different normalization regression models were developed (one for each of three bands per image times four images) which relate pixel DNs for images to be normalized with those of the reference image. The normalization equations for the 11 May 1987 scene are shown in Figure 2. Each regression model contains an additive component that corrects for the difference in atmospheric path radiance between dates, and a multiplicative term that corrects for the difference in detector calibration, sun angle, Earth/sun distance, atmospheric attenuation, and phase angle between dates. After application of these normalization regression models, the 1987 and 1988 images were ready for transformation into Brightness and Greenness spectral features, and classification into irrigated and not irrigated classes.

Prior to selection of the empirical normalization technique, another more simple method of normalization, which we call "deterministic," was investigated. This method will be described briefly, and its results compared with those of the empirical technique. This comparison is presented to illustrate the effects of atmospheric and phase angle differences on SPOT HRV images, and to demonstrate the strengths of the empirical normalization technique.

The deterministic normalization method obtains the additive term (path radiance correction) from a constant, near zero reflectance target in the image, and calculates the multiplicative term from detector calibration, sun angle, and Earth/sun distance data (Appendix). This method requires less analyst interaction with the image than the empirical technique because scene DNs are used only to develop an estimate of path radiance. The drawbacks to this approach are that it ignores differences in atmospheric attenuation and phase angle between dates. In the arid, high desert environment of the Newlands Project, atmospheric attenuation might sometimes be ignored without major adverse impacts. However, the 50° differences in view angle between east- and west-looking SPOT HRV acquisitions make the Lambertian assumption a significant problem. Moran *et al.* (1990) showed that reflectances of agricultural crops can vary by over 10 percent when look angle varies by 33 degrees (23° east to 10° west).

Table 4 shows the differences between the multiplicative normalization coefficients derived using the empirical and the deterministic techniques. There is a trend for the empirically derived multiplicative terms to be higher than the deterministically derived terms for scenes that were acquired looking left (east), but lower for the scenes acquired looking right (west). This effect can be at least partially explained by increased microrelief shadowing at eastward look angle in the bright normalization targets used to develop the empirical normalization equations. Shadows from microrelief make up a larger portion of any given pixel when a sensor is looking towards the illumination source than when it is looking away from the illumination source (Hapke, 1981; Pinty *et al.*, 1989). Shadowing reduces the DNs associated with bright normalization targets, thereby requiring application

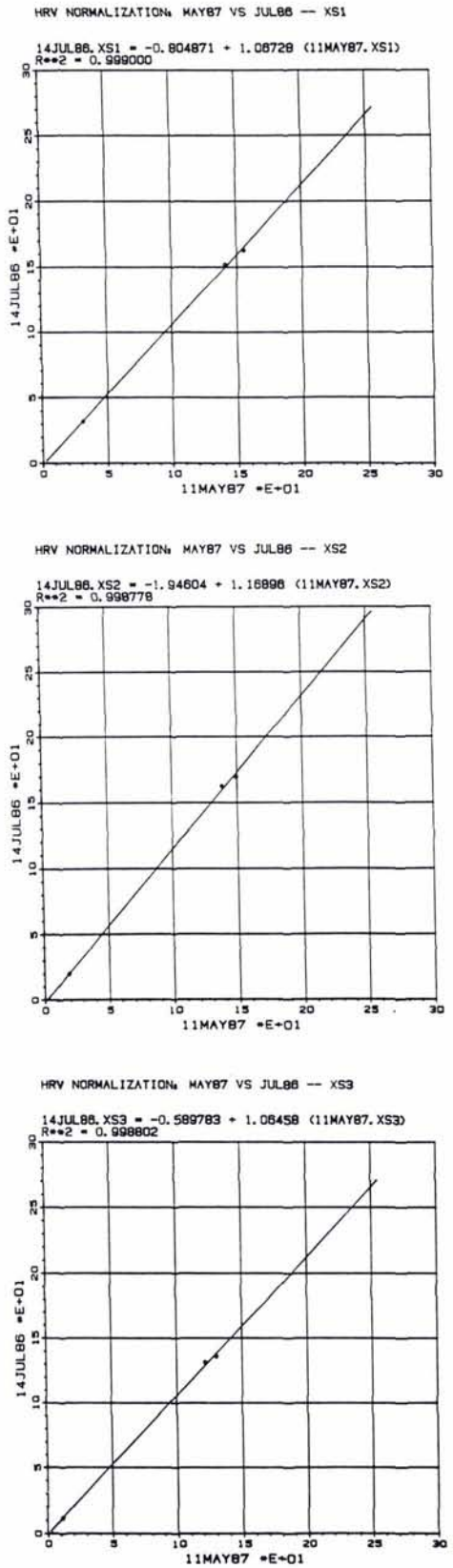

FIG. 2. Normalization equations for the 11 May 1987 HRV scene.

of a larger multiplicative term to normalize these targets to their counterparts on the reference scene.

The effect of increased atmospheric attenuation at the shorter wavelengths can also be seen in Table 4. for the scenes acquired with a left (east) look angle (11 May 1987 and 21 August 1988), the difference between the empirically and deterministically derived multiplicative terms is greatest for the shorter wavelength bands. The reduced dynamic range caused by atmospheric attenuation compounds the effect of reduced dynamic range caused by increased shadowing. This requires increasingly greater correction factors as wavelength decreases from XS3 to XS1. For the scenes acquired with a right (west) look angle (14 August 1987 and 21 May 1988), the difference between empirically and deterministically derived multiplicative terms is lowest in the shorter wavelength bands. The reduced dynamic range caused by atmospheric attenuation counteracts the increased dynamic range resulting from reduced shadowing, relative to the shadowing conditions of the 14 July 1986 normalization standard.

Moran *et al.* (1990) used hand-held radiometer data to show that empirical view angle corrections developed from bare soil targets significantly reduce view angle related radiance variations over agricultural crop canopies. The empirical normalization equations developed in this study appear to have the same effect. Visual comparison of normalized 1987 and 1988 HRV images showed that images normalized using the empirically derived normalization equations more closely resembled the reference scene than images normalized using the deterministically derived equations. The compensation for microrelief shadowing built into the empirical technique appears to at least partially compensate for shadowing within the desert scrub and alfalfa canopies that dominate the HRV scenes.

Image Transformation

Study of multispectral HRV imagery has shown that there is a high degree of correlation between bands (Table 5). The three-band HRV images were transformed into two uncorrelated, physically relevant spectral features called Brightness and Greenness (Jackson, 1983; Kauth and Thomas, 1976; Verdin *et al.*, 1987). Brightness values correspond to general surface brightness, while Greenness values correspond to amount of photosynthetically active green vegetation present. These features are linear combinations of the three raw bands (Equations 1 and 2), and represent an axis rotation of the original data (Figure 3).

Equation 1. Brightness for 14 July 1986 HRV data:

$$\text{Brightness} = 0.60539\,(\text{XS1}) + 0.61922\,(\text{XS2}) + 0.50008\,(\text{XS3})$$

Equation 2. Greenness for 14 July 1986 HRV data:

$$\text{Greenness} = -0.30132\,(\text{XS1}) - 0.40321\,(\text{XS2}) + 0.86408\,(\text{XS3})$$

Brightness and Greenness images typically preserve most of the information present in the raw data while reducing data volume by one-third.

The Brightness and Greenness equations listed in Equations 1 and 2 were developed from the July 1986 HRV scene. Equations 1 and 2 were algebraically combined with the appropriate scene normalization equations before being applied to the 1987 and 1988 HRV scenes. Brightness images contained real numbers with ranges exceeding 255, and Greenness images contained negative real numbers. To reduce data handling costs,

TABLE 4. COMPARISON OF MULTIPLICATIVE TERMS FROM EMPIRICALLY AND DETERMINISTICALLY DERIVED NORMALIZATION EQUATIONS.

Reference Scene:	Date = 14 July 1986 Sensor = HRV2 Look angle = L 1.7°			
	Band	Empirical	Deterministic	Difference
Date: 11 May 1987	XS1	1.06728	1.01469	0.05259
Sensor: HRV1	XS2	1.16896	1.12115	0.04781
Look angle: L 20.2°	XS3	1.06458	1.03217	0.03241
Date: 14 August 1987	XS1	1.06704	1.06206	0.00498
Sesor: HRV2	XS2	1.05145	1.06206	−0.01061
Look angle: R 22.3°	XS3	1.02591	1.06206	−0.03615
Date: 21 May 1988	XS1	0.98373	1.01246	−0.02873
Sensor: HRV2	XS2	0.97683	1.01246	−0.03563
Look angle: R 27.2°	XS3	0.94976	1.01246	−0.06270
Date: 21 August 1988	XS1	1.23026	1.06957	0.16069
Sensor: HRV1	XS2	1.30678	1.18178	0.12500
Look angle: L 20.9°	XS3	1.19531	1.08799	0.10732

TABLE 5. CORRELATION MATRIX FOR A SUBSET OF THE 21 MAY 1988 HRV SCENE.

	HRV1	HRV2	HRV3
HRV1	1.00		
HRV2	0.99	1.00	
HRV3	0.30	0.24	1.00

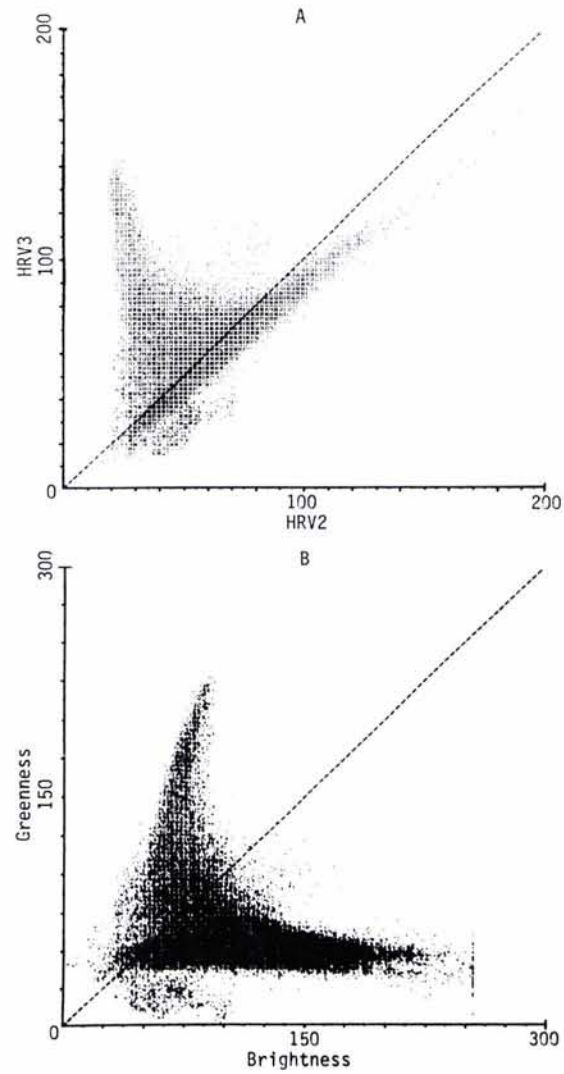

FIG. 3. Bispectral plots from the 21 August 1988 HRV scene. A: HRV2 vs HRV3 B: Brightness vs. Greenness

these images were remapped from real to byte format as shown in equations 3 and 4.

Equation 3.

$$\text{Brightness}^* \{\text{byte}\} = -35 + 1.466\ (\text{Brightness}\{\text{real}\})$$

Equation 4.

$$\text{Greenness}^* \{\text{byte}\} = 34 + 1.457\ (\text{Greenness}\ \{\text{real}\})$$

Pixel-by-Pixel Classification

Individual pixels were classified as irrigated or not irrigated using Greenness and Brightness thresholds. Threshold values were chosen with the aid of Reclamation staff who are very familiar with the study area and the agricultural practices employed there. Pixels with Greenness values above a minimum Greenness threshold were identified as having a significant amount of green vegetation, indicating irrigation, while pixels with Brightness values below a maximum Brightness threshold were identified as having dark, moist soil, indicating recent application of irrigation water.

To obtain an "irrigated" attribute, a field had to be identified as irrigated on either the May scene or the August scene (or both). To facilitate the classification procedure, Composite Greenness (CG) and Composite Brightness (CB) images were derived from the Greenness and Brightness images from the May and August scenes for each year. Each pixel in the CG image contained the higher of the two corresponding Greenness values from the two parent images. Similarly, each pixel in the CB image contained the lower of the two corresponding Brightness values from the two parent images.

Reclamation personnel developed the CG and CB threshold values by studying limited per-field irrigation data available for a small part of the study area, 1:12,000-scale color infrared aerial photography acquired in 1984, and the 1987 and 1988 HRV imagery. The 1984 photography provided information about soil color, soil conditions, and location of water conveyance structures that was used to complement the information available from the HRV color composites. Results of preliminary classifications were studied, and the threshold values were modified until an optimal classification was achieved. Each pixel was classified into one of four classes:

- IRRGRN- identified as irrigated by high CG: $CG \geq 85$ (higher Greenness is associated with higher amounts of green vegetation)
- IRRBRT- identified as irrigated by low CB: $0 < CB \leq 80$ (lower Brightness is associated with moister, darker soils)
- NOIRR- not irrigated: $CG < 85$ AND $CB > 80$
- NOIMAGRY- partial or missing image coverage: $CB = 0$

There were some problems associated with this classification procedures. Dark, moist soils have been shown to decrease the Greenness values of partial canopy vegetation compared to the same vegetation on dry soil backgrounds (Huete *et al.*, 1984; Huete *et al.*, 1985). This meant that the CG threshold might identify some pixels with a moderate vegetation density on a dry soil background as being irrigated, while identifying pixels with the same vegetation density on a darker soil background as being not irrigated. This problem was ameliorated somewhat by the CB threshold which identified those pixels with moist soils as being irrigated. Another problem was the variability in soil types across the study area. Freshly plowed lands in the clay-rich soils in the northeast part of the study area had approximately the same CB values as wet soils in other parts of the study area. This led to commission errors (calling non-irrigated land irrigated) for portions of the northeast part of the study area.

*Values are rounded to whole numbers, and are truncated at 0 or 255 if they exceed byte range.

Overlay Analysis

Irrigated land area estimates could have been derived by simply counting the number of pixels in the study area that were classified as irrigated by the CG and CB thresholds. However, inconsistent vegetation cover within agricultural fields due to non-uniform soil conditions, pest attacks, or irrigation water applications can cause some pixels within irrigated fields to be identified as not irrigated. Similarly, pixels occurring on edges of agricultural fields can either overestimate or underestimate total irrigated area depending upon vegetation canopy cover and threshold values. Furthermore, some non-irrigated features such as riparian vegetation can be identified as irrigated land.

These problems were avoided by employing the Newlands GIS in the acreage estimation procedure. Instead of counting HRV pixels to obtain total irrigated area, the HRV imagery was used only to provide an irrigated or not irrigated attribute for each individual agricultural field stored within the GIS. This was done by overlaying rasterized field boundaries from the GIS onto the classified HRV imagery, and applying the following decision rules to the aggregate of pixels contained within each field:

Not Irrigated: (IRGRNPCT + NOIMPCT) < 33% OR NOIRRPCT > 50%
attribute = 0

Irrigated: IRGRNPCT ≥ 33% AND (IRGRNPCT + IRBRTPCT) ≥ 50%
attribute = 1

Unknown: all other cases
attribute = 2

where

IRGRNPCT = percentage of pixels identified as irrigated by the CG threshold,
IRBRTPCT = percentage of pixels identified as irrigated by the CB threshold,
NOIRRPCT = percentage of pixels meeting neither the CG or CB thresholds, and
NOIMPCT = percentage of pixels with no image coverage.

To be identified as irrigated, a field had to have at least 33 percent of its pixels classified as irrigated by the CG threshold, and at least a combined 50 percent by the CG and CB thresholds. Fields receiving an "irrigated" attribute were required to have at least 33 percent of their pixels classified as irrigated by the CG threshold to avoid calling freshly plowed fields in the northeast part of the study area irrigated when they in fact were not.

Once the agricultural field data layer contained irrigation attributes for 1987 and 1988, it could be combined with any of the other data layers within the GIS to provide estimates of maximum irrigation water demand, and other information.

Results

Accuracy assessment was performed by one of the Reclamation staff members from the Sacramento Office who helped develop the classification procedure. The same ground reference information, aerial photography, and HRV imagery that were used for classifier development were used for accuracy assessment. Performance of the irrigated lands classifier appears to be very good (Table 6). For the majority of fields identified as being irrigated, irrigation status was obvious. These fields were not reinterpreted by the analyst performing the accuracy assessment. However, accuracy was checked on fields with questionable irrigation status. These fields were defined as those having 0 to 70 percent irrigated pixels (as defined by both the CG and CB thresholds). For both years, these fields amounted to about 20 percent of the fields classified for the year. Reevaluation of the attributes assigned by the automated classifier led to a reversal of the automated classification for 146 fields amounting to 791 hectares for 1987 (2.8 percent of the total number of fields and 2.9 percent of the total potentially irrigated area for which image coverage was available) and 132

TABLE 6. CONFUSION MATRICES FOR THE 1987 AND 1988 Automated Classifications (in Hectares).

1987		Actual: Irrigated	Nonirrigated	Total
Classified as:	Irrigated	24,593	133	24,726
	Nonirrigated	658	1,526	2,184
	Total	25,251	1,659	26,910
	Percent correct	97.4	92.0	

1988		Actual: Irrigated	Nonirrigated	Total
Classified as:	Irrigated	23,411	100	23,511
	Nonirrigated	456	2,107	2,563
	Total	23,867	2,207	26,074
	Percent correct	98.1	95.5	

fields accounting for 556 hectares for 1988 (2.7 percent of the total number of irrigated fields and 2.1 percent of the total potentially irrigated area for which image coverage was available). Stated conversely, the automated classifier was found to be better than 97 percent correct for both areal coverage of irrigated land and number of fields being irrigated for both 1987 and 1988.

Although these results are good, there is room for improvement. Upon inspection of the automated classifier results, Reclamation staff noticed problems the classifier had in dealing with very small fields, grain fields planted in the spring, and marshy pasture lands. Small fields (less than one-half hectare) were occasionally misclassified due to misregistration of the agricultural field mask onto the classified imagery. Whereas slight misregistrations are inconsequential when determining the irrigation status of larger fields, these misregistrations can be very serious in small fields due to the increased proportion of edge pixels. This problem can be remedied only through better image registration, or increasing the minimum field size stored in the GIS.

The majority of the omission errors (identifying an irrigated field as not irrigated) occurred in some spring grain fields and in marshy pasture lands in the northeast portion of the study area. The spring grain fields failed to meet the Greenness threshold in May because they did not exhibit enough emergent vegetation, and failed in August because they had already been harvested and burned. The marshy pasture lands failed to meet the Greenness threshold for either date because the discontinuous grassy vegetation cover growing over a moist to very wet clay soil failed to produce a large enough Greenness signal. Although nearly all of these fields contained a majority of pixels meeting the CB threshold, these fields lacked enough pixels meeting the CG threshold (33 percent) to be identified as irrigated. To improve classifier performance, future work may include stratification of the study area into at least two distinct soil classes with dirrerent irrigation attribute decision rules for each soil class.

IDENTIFYING PREVIOUSLY UNMAPPED IRRIGATED FIELDS

Because the agricultural field boundaries present in the Newlands digital geographic data base were derived from aerial photography acquired in 1984, the potential exists for new lands to have been brought into production since that time. The procedure described above is only capable of assigning irrigation attributes to agricultural fields that are already present in the GIS. An image product was generated that allowed for identification of lands brought into production since 1984.

This new image product was generated by overlaying an image mask showing the locations of all agricultural fields onto the CG images for 1987 and 1988. The resulting images showed fields present in the Newlands GIS in black against a CG image background, with increasing CG values from black to white (Figure 4). Agricultural fields brought into production since 1984 appear as unobscured, bright, rectangular areas (Figure 5).

New agricultural fields identified by this procedure were outlined on 1:12,000-scale aerial photographs using contextual clues such as roads, fence lines, or irrigation ditches as guides. These fields were transferred to orthophoto quadrangles and digitized into the Newlands Project GIS.

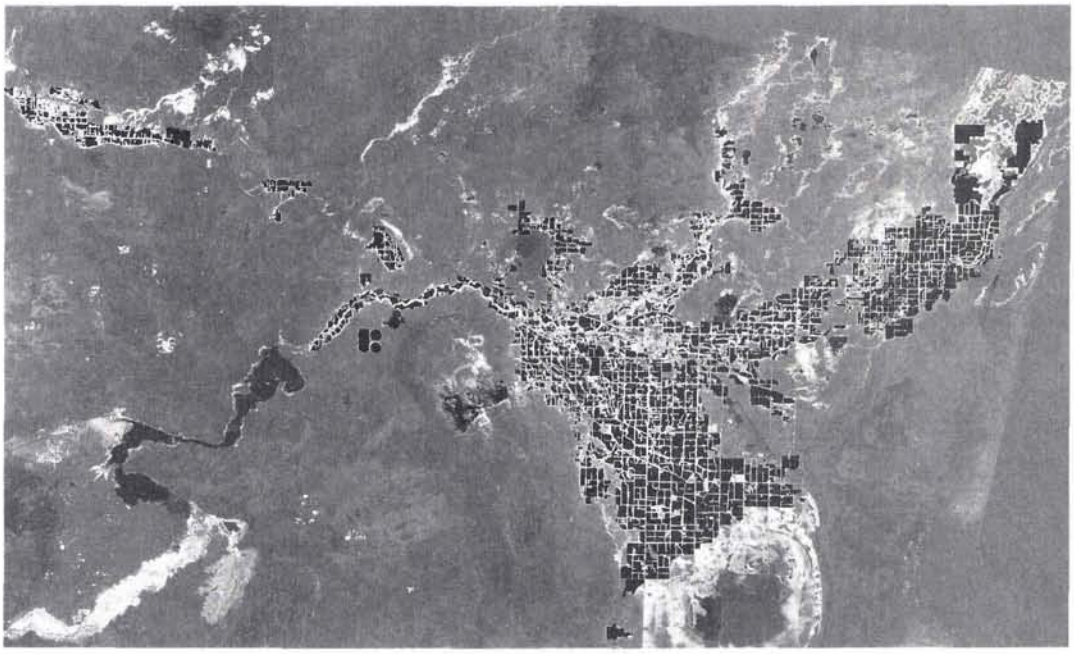

FIG. 4. Composite greenness image for 1988 with previously digitized agricultural fields shown in black. Increasing grey tones indicate increasing amount of green vegetation.

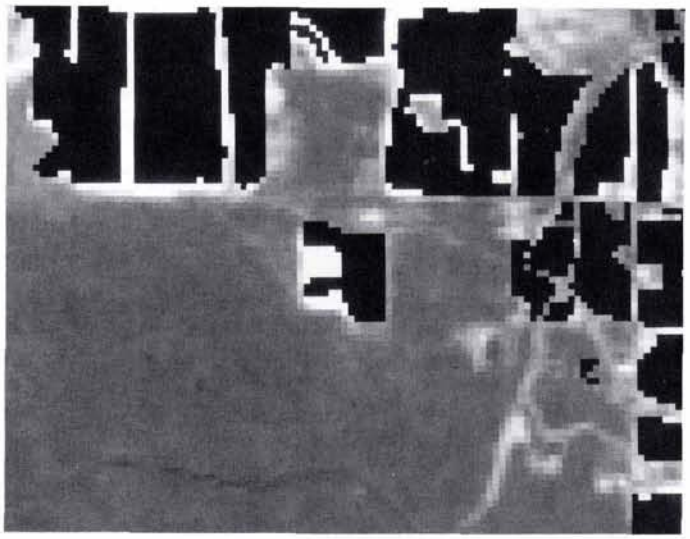

FIG. 5. An enlargement of a portion of Figure 4 showing an agricultural field brought into production since field boundaries were initially digitized in 1984.

DISCUSSION

This project illustrates how imagery acquired by spaceborne sensors can be merged with accurate spatial information contained within a GIS to generate information useful to irrigated lands managemet. As is typical with information systems of this type, the Newlands GIS is finding valuable use beyond that for which it was originally designed. For example, the U.S. Fish and Wildlife Service is using the GIS to help identify actively irrigated, water righted land whose water might be purchased and used to enhance wildlife habitat in the Stillwater National Wildlife Refuge, which is adjacent to and downstream of the project. The GIS is also furnishing valuable basic data to studies of consumptive use and irrigation effiency in the project. The Newlands Project GIS stands as an excellent example of the support that remote sensing and GIS can bring to water resource management.

REFERENCES

Centre National d'Etudes Spatiales (CNES), 1988. *SPOT User's Handbook*, Volume 1. CNES and SPOT Image Corporation, Toulouse, France, 272 p.

Jackson, R. D., 1983. Spectral Indices in n-Space, *Remote Sensing of Environment*. 13:409–421.

Kauth, R. J., and G. S. Thomas, 1976. Tasseled Cap - A Graphic Description of the Spectral-Temporal Development of Agricultural Crops as Seen by Landsat. *Proceedings of the Symposium on Machine Processing of Remotely Sensed Data*, Purdue University, West Lafayett, Indiana, pp. 4B41–4B51.

Hapke, B., 1981. Bidirectional Reflectance Spectroscopy 1. Theory, *Journal of Geophysical Research*. 86(B4):3039–3054.

Huete, A. R., D. F. Post, and R. D. Jackson, 1984. Soil Spectral Effects on 4-Space Vegetation Discrimination, *Remote Sensing of Environment*. 15:155–165.

Huete, A. R., R. D. Jackson, and D. F. Post, 1985. Spectral Response of a Plant Canopy with Different Soil Backgrounds, *Remote Sensing of Environment*. 17:37–53.

Moran, M. S., R. D. Jackson, G. F. Hart, P. N. Slater, R. J. Bartell, S. F. Biggar, D. I. Gellman, and R. P. Santer, 1990. Obtaining Surface Reflectance Factors from Atmospheric and View Angle Corrected SPOT-1 HRV Data, *Remote Sensing of Environment*. (in press).

Pinty, B., M. M. Verstraete, and R. E. Dickenson, 1989. A Physical Model for Predicting Bidirectional Reflectances over Bare Soil, *Remote Sensing of Environment*. 27:273–288.

Verdin, J. P., 1983. Corrected Versus Uncorrected Landsat 4 MSS Data: A Brief Comparison, *Landsat Data Users Notes*. No. 27, pp. 4–8.

Verdin, J. P., M. P. Crane, and G. P. Lyford, 1985. Application of a Digital Geographic Data Base to Irrigation Water Rights Management, *Remote Sensing Applications for Consumptive Use (Evapotranspiration)*, American Water Resources Association, Bethesda, Maryland, pp. 35–49.

Verdin, J. P., D. W. Eckhardt, and G. R. Lyford, 1987. Evaluation of SPOT Imagery for Monitoring Irrigated Lands, *Proceedings of the SPOT 1 Image Utilization, Assessment, Results Symposium*, Paris, France, pp. 81–91.

(Received 16 October 1989; accepted 18 December 1989; revised 9 March 1990)

APPENDIX
DETERMINISTIC SCENE NORMALIZATION

Let:

D	= Dark normalization target DN
1/A	= radiance interval between successive DN counts (from scene header information). Smaller A values indicate smaller dynamic ranges for a given radiance range.
θz	= solar zenith angle
ES	= Earth/sun distance
ref	= reference scene
norm	= scene being normalized

Multiplicative correction term (M):

$$M = \frac{(\cos \theta z_{ref})(1/ES^2_{ref})(A_{ref})}{(\cos \theta z_{norm})(1/ES^2_{norm})(A_{norm})}$$

Additive correction term (C):

$$C = D_{ref} - (D_{norm})\,(M)$$

Example:

Reference scene:

Date = 14 July 1986, Sensor = HRV2, Band = XS2
D = 20, θz = 22.6°
A = 0.45, ES = 1.0165263

Scene to be normalized:

Date = 11 May 1987, Sensor = HRV1, Band = XS2
D = 19, θz = 23.9°
A = 0.40, ES = 1.0098497

$$M = \frac{(\cos(22.6))(1/(1.0165263)^2)(0.45)}{(\cos(23.9))(1/(1.0098497)^2)(0.40)} = 1.12115$$

$$C = 20 - 19(1.12115) = -1.30179$$

So, $DN_{ref} = -1.302 + 1.121\,(DN_{norm})$